THE JOURNAL OF PHYSICAL CHEMISTRY A
A JOURNAL OF THE AMERICAN CHEMICAL SOCIETY

Exploring the Nature of Anion−π Interactions: Complexes of π-Acceptors with Fluoro- or Oxoanions Compared to the Associations with Halides

Favour E. Odubo, Matthias Zeller, and Sergiy V. Rosokha*

Cite This: https://doi.org/10.1021/acs.jpca.3c02704 Read Online

ACCESS | Metrics & More | Article Recommendations | Supporting Information

ABSTRACT: The variations in the nature and properties of the anion−π complexes with different types of anions are identified via experimental (UV−vis and X-ray crystallographic) measurements and computational analysis of the associations of tetracyanopyrazine, tetrafluoro-, or dichlorodicyano-*p*-benzoquinone. Co-crystals of these π-acceptors with the salts of fluoro- and oxoanions (PF_6^-, BF_4^-, $CF_3SO_3^-$, or ClO_4^-) comprised anion−π bonded alternating chains or 1:2 complexes showing interatomic contacts of up to 15% shorter than the van der Waals separations. DFT computations confirmed that binding energies between the neutral π-acceptors and polyatomic noncoordinating oxo- and fluoroanions are comparable to those in the previously reported anion−π complexes with more nucleophilic halides. Yet, while the latter show distinct charge-transfer bands in the UV−vis range, the absorption spectra of the solutions containing oxo- and fluoroanions and the π-acceptors were close to those of the individual reactants. The natural bond orbital (NBO) analysis revealed a very small charge transfer of Δq = 0.01−0.02 e in the complexes with oxo- or fluoroanions as compared to the Δq = 0.05−0.22 e found for analogous complexes with halides. These distinctions were related to the smaller frontier orbital energy gap and better overlap in the complexes with halides (since the highest occupied orbitals of these monoatomic anions are closer in energy to the lowest unoccupied orbitals of the π-acceptors) as compared to that in the multicenter-bonded associations with polyatomic oxo- and fluoroanions. In accordance with these data, the energy decomposition analysis showed that while the complexes of neutral π-acceptors with the fluoro- and oxoanions are formed predominantly via electrostatic interaction, the associations with halides comprised significant orbital (charge-transfer) interactions and they explain their spectral and structural features.

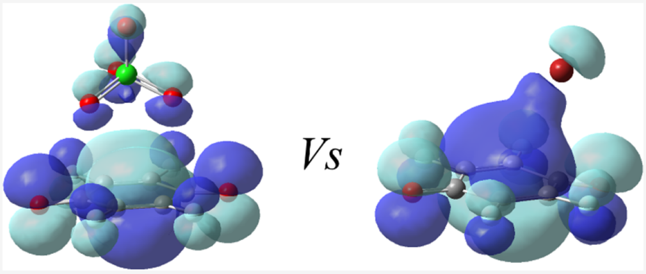

1. INTRODUCTION

During the last two decades, the studies of anion−π interaction advanced from the discovery of the computational evidence of the attraction of anions to electron-deficient π-systems[1−3] to its experimental observations and utilizations for anion recognition and transport, crystal engineering, and catalysis.[4−10] Most commonly, this interaction is related to the attraction of anions to the area of the positive electrostatic potential on the surface of π-systems perpendicular to its molecular framework, referred to as π-holes.[11] However, a few computational investigations brought about arguments that it is related to the interaction of anions with the electronegative substituents in the aromatic ring[12,13] or that it should be called anion−σ interaction.[14] There were also indications of the charge-transfer character or multicenter covalency of the anion−π bonding.[15−20] Indeed, an analysis of the X-ray crystallographic (solid-state) data revealed drastic variations in the modes of the anion−π bonding ranging from η^6 interaction of anions located over the center of the aromatic ring to their η^1 binding with one of the atoms of the π-acceptor.[9,17] Also, an addition of halides to the solutions of π-acceptors frequently resulted in the change of color of the mixtures, suggesting a substantial role of charge-transfer (molecular orbital) interactions in the formation of anion−π complexes in such systems.[18−21] While a similar change of color was found in the analogous systems with thiocyanate, nitrate, and iodometallates,[16,22] no such effects were observed with many other polyatomic anions (e.g., hexafluorophosphate or anionic metal-halide complexes).[22−25] The diverse structural and spectral features of the anion−π complexes (related to the wide variations of the properties of the anions and π-systems) suggest the possibility of substantial differences in the nature of their interactions.[16]

While the nature of anion−π bonding and its major components were explored in a number of the earlier studies,[1−3,12−15,26−31] the distinctions related to the variation

Received: April 25, 2023
Revised: June 17, 2023

of anions in such systems are still inconclusive. For example, a recent extensive energy decomposition analysis revealed variations in the strength of interaction and contributions of electrostatics and London dispersion components in a number of the complexes of different anions with heterocalixarene of cyclophane-based π-receptors.[30] The multicenter bonding in such systems is well-suited for molecular recognition.[7,24] The strengths of the interaction of the complexes of such macrocyclic hosts were governed, however, mostly by the structural fit of the anions to the cavity of the receptors.

To clarify the distinctions, if any, in the nature of the bonding involving different anions, we analyze in the current work anion−π complexes of tetracyanopyrazine, tetrafluoro-, and dichlorodicyano-*p*-benzoquinones (which are shown together with their acronyms in Chart 1) with the fluoro- and oxoanions (PF_6^-, BF_4^-, $CF_3SO_3^-$, and ClO_4^-) and compared their properties with those of the similar associations with halides.

Chart 1. Structures and Acronyms of the π-Acceptors

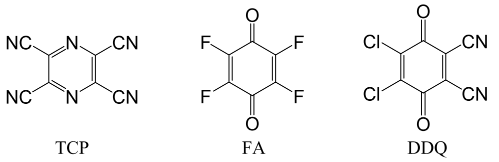

The molecules in Chart 1 are strong electron acceptors with reduction potentials of −0.20, 0.02, and 0.56 V vs SCE for TCP, FA, and DDQ, respectively.[20,32] The literature data indicated the propensity of these neutral π-acceptors to binding (pseudo)-halides, metal halides, and other anions.[18,20,21,33,34] In particular, the study of complexes of TCP with halide (Cl^-, Br^-, and I^-) anions provided evidence of anion−π bonding in solution and the solid state.[18] The Mulliken dependence of the energy of the absorption bands, which was observed for the complexes of TCP and *p*-benzoquinones with (pseudo-)halides suggested the charge transfer nature of such associations.[16,18] In the systems in which the strongest π-acceptors (e.g., DDQ) were combined with the I^- or Br^- anions (which are rather strong electron donors), the formation of the charge-transfer complexes was followed by electron transfer.[20]

In contrast to halides, the fluoro- and oxoanions are noncoordinating polyatomic species. They are very weak bases and poor nucleophiles and reducing agents. As such, they are frequently used as the anionic parts of the supporting electrolytes providing a supposedly inert environment for the measurements of the reactions of ionic species. Yet, utilization of the Bu_4NPF_6 salt for the study of the salt effects in anion−π interactions indicated comparable strengths of the bonding of PF_6^- and halide anions with *p*-benzoquinone derivatives.[35] The literature also contains reports on anion−π bonding of fluoro- or oxoanions with polydentate receptors or tetrazine derivatives, which were studied in presence of halide anions.[31] However, there are essentially no data about similarities and differences, if any, in nature and properties of anion−π complexes of these polyatomic weakly coordinating anions as compared to analogous associations involving more nucleophilic monoatomic halides. As such, in the current work, we establish structural, spectral, and thermodynamic features of the complexes of BF_4^-, PF_6^-, $CF_3SO_3^-$, and ClO_4^- anions with TCP, FA, and DDQ π-acceptors. These experimental measurements are followed by the computational analysis of the bonding in such associations side by side with their analogs formed by the same π-acceptors with halide anions. The distinctive characteristics of halides vs fluoro- and oxoanions suggest that the comparison of their anion−π complexes will assist in establishing components of anion−π bonding and will provide insight into the nature of such interactions. In addition, the study of the complexes of π-acceptors in Chart 1 will allow examining distinctions (if any) and trends in anion−π bonding related to the variation of the nature (aromatic and benzoquinone) and electron-acceptor strength of the π-acceptors.

2. METHODS

Tetrafluoro-*p*-benzoquinone, dichlorodicyano-*p*-benzoquinone, tetracyanopyrazine, and tetraalkylammonium salts of halides, hexafluorophosphate, tetrafluoroborate, triflate, and perchlorate were purified by recrystallization. $[K(crp)]PF_6$ and $[K(crp)]BF_4$ (crp = [2.2.2]cryptand) were prepared by interaction of KPF_6 or KBF_4 with crp in methanol; Pr_4NPF_6 was prepared by the neutralization of a solution of Pr_4NOH with HPF_6. Dichloromethane and acetonitrile were distilled over P_2O_5 under an argon atmosphere.

Single crystals of $(Pr_4N)PF_6{\cdot}DDQ$, $(Pr_4N)BF_4{\cdot}DDQ$, $(Bu_4N)CF_3SO_3{\cdot}DDQ$, $(Pr_4N)ClO_4{\cdot}DDQ$, $(Pr_4N)PF_6{\cdot}FA$, $(Pr_4N)BF_4{\cdot}FA$, $(Pr_4N)ClO_4{\cdot}FA$, $[K(crp)]PF_6{\cdot}TCP$ and $[K(crp)]BF_4{\cdot}TCP$ were prepared by cooling acetonitrile solutions containing equimolar quantities of the corresponding π-acceptor and the salt from room temperature to −30 °C. The X-ray measurements were carried out on a Bruker AXS D8 Quest diffractometer with a molybdenum radiation X-ray tube ($\lambda = 0.71073$ Å). Reflections were indexed and processed, and the files were scaled and corrected for absorption using APEX3.[36] The structures were solved by direct methods using XPREP within the SHELXTL suite of programs and refined by full-matrix least-squares against F^2 with all reflections using Shelxl2016 with the graphical interface Shelxle.[37−39] Crystallographic, data collection, and structure refinement details are listed in Table S1 in the ESI. Complete crystallographic data, in CIF format, have been deposited with the Cambridge Crystallographic Data Centre. CCDC 2256203−2256211 contain the supplementary crystallographic data for this paper. These data can be obtained free of charge via www.ccdc.cam.ac.uk/data_request/cif.

The formation of complexes between anions and π-acceptors was studied at 22 °C via UV−vis measurements of the series of solutions with constant (2−10 mM) concentrations of a π-acceptor and variable concentrations (from 0 to 0.4 M) of anions. The effective formation constants, K_{eff}, were obtained via regression analysis of the differential intensities of absorption, ΔAbs (obtained by the subtraction of absorption of components from the absorption of their mixtures), for these series as described earlier (see the Supporting Information for details).[35]

Geometries of the complexes were optimized without constraints via M062X/def2tzvpp calculations using the Gaussian 09 suite of programs.[40−42] For comparison with the experimental measurements, calculations were done in dichloromethane using a polarizable continuum model.[43] The absence of imaginary frequencies confirmed that the optimized structures represent true minima. An earlier analysis demonstrated that intermolecular associations are well-modeled using this method.[44] The M062X functional provided the most reliable results among several density functionals in the analysis of anion−π interactions.[45] The def2tzvpp basis set does not include a diffuse function since previous analysis demonstrated that very similar results were obtained in the modeling of noncovalent interactions involving anions with the triple-ζ basis sets with and without diffuse functions.[46] Our previous studies also showed that M062X/def2tzvpp calculations reproduced well experimental features of the anion−π complexes.[16,20] Binding energies, ΔE_b were determined as: $\Delta E_b = E_C - (E_A + E_X)$, where E_C, E_A, and E_X are sums of the electronic and ZPE of the optimized complex, π-acceptor, and anion. Since the formation of the complex is accompanied by distortion of the reactants, the binding energy represents a combination of preparation (distortion) energy, E_{prep}, and interaction energy between distorted fragments, ΔE_{int}. UV−vis spectra were obtained via TD-DFT calculations, and charge transfer values, Δq, were estimated via natural bond orbital (NBO) calculations.[47] Quantum theory of atoms in molecules (QTAIM)[48,49] and noncovalent indices (NCI)[50] analyses were performed with Multiwfn and visualized using VMD programs.[51,52] (The NCI setting was: isovalue = 0.5, color-coded with sgn(λ_2)ρ in the range from −0.04 a.u. (blue, strong attractive interaction) to 0.02 a.u. (red, strong nonbonded overlap). Energy decomposition analyses (EDA) were carried out using the Amsterdam density functional (ADF) of the Amsterdam Modeling Suite[53−55] via single-point calculations with the B3LYP-D3 functional (since it allowed evaluation of the dispersion component of the interaction energy) and the TZ2P basis set available in AMS using atomic coordinates of the complexes optimized as described above (EDA analysis with the PB86-B3(BJ) functional produced similar results).

3. RESULTS AND DISCUSSION

3.1. X-ray Structural Analysis of the Anion−π Associations.

A strong tendency of DDQ, FA, or TCP to bind fluoro- and oxoanions was first established via X-ray structural studies of their associations in the solid state. Indeed, slow cooling of the solutions containing equimolar quantities of any of these π-acceptors and a salt of the PF_6^-, BF_4^-, ClO_4^-, or $CF_3SO_3^-$ anion with bulky tetraalkylammonium or cryptand-encapsulated potassium cations resulted in the formation of crystals comprising both these components. X-ray structural analysis showed that these co-crystals contained, in most cases, one-dimensional (1D) stacks of the π-acceptors alternately interspersed with the π-bonded anions, as illustrated in Figure 1 and Figures S1−S5 in the Supporting Information.

Similar to the reported earlier stacks formed by TCP with planar or tetrahedral halometallate anions,[22−24] these chains show parallel arrangements of every other π-acceptor, which were somewhat tilted relative to the normal plane of the vertical axes of the 1D associations. Within the latter, anions were nested between the planes of the π-acceptors, and several interatomic contacts between neighbors were shorter than their van der Waals separations. The anions were well separated from the bulky tetraalkylammonium counter-ions (Figures S1−S5 in the Supporting Information). The only exception was observed in the co-crystals of TCP with [K(cryptand)]PF_6, in which PF_6^- anions were coordinated to potassium cation (Figure 1B). Yet, the general arrangements of the anions and π-acceptors in these π-bonded alternating chains were similar to those observed in the 1:1 crystals with tetraalkylammonium counter-ions.

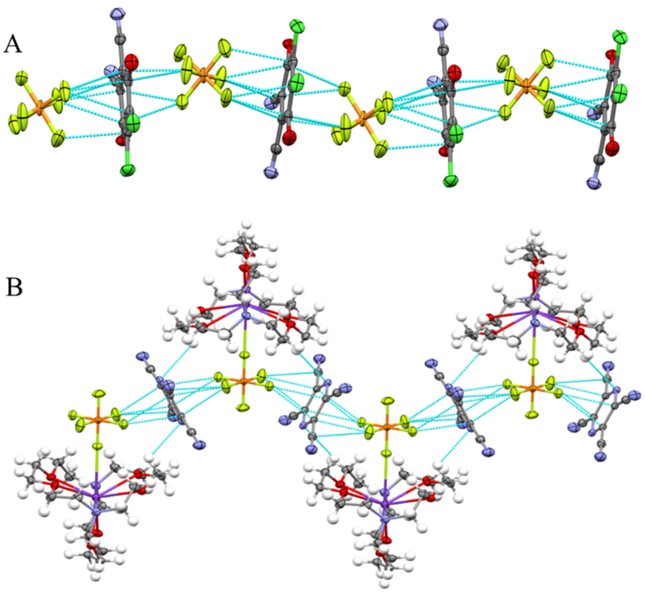

Figure 1. Segments of the 1D anion/π-acceptor stacks in the co-crystals of (A) DDQ with $(Pr_4N)PF_6$ (the counter-ions are not shown, for clarity) and (B) TCP with [K(crp)]PF_6. Light blue lines show intermolecular contacts, which are shorter than the van der Waals separations. Atom color code: white, hydrogen; gray, carbon; red, oxygen; blue, nitrogen; green, chlorine; orange, phosphorus; chartreuse, fluorine.

Besides 1D chains, co-crystallization of FA with Pr_4NClO_4 or Pr_4NBF_4 produced discrete 1:2 complexes as illustrated in Figure 2. The π-acceptors in these associations also show several contacts shorter than the van der Waals separations with both their anionic counterparts. The characteristics of the closest contacts between the anions and π-acceptors are listed in Table 1.

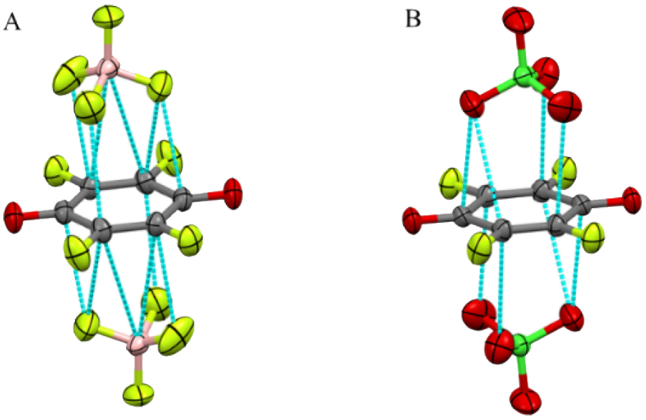

Figure 2. X-ray structures of 1:2 complexes of FA with BF_4^- (A) and ClO_4 (B) anions (color code is the same as in Figure 1).

The consistent formations of co-crystals between DDQ, FA, and TCP molecules and ionic salts of oxo- and fluoroanions showing close contacts between anions and neutral π-acceptors indicated a strong interaction between these species. These facile co-crystallizations were analogous to those observed with the halide salts.[18,20] All these associations comprised multiple interatomic contacts with the distances between neighboring anions and π-acceptors $d_{X\cdots C}$, which were noticeably shorter than the sum of the corresponding van der Waals radii, $r_X + r_C$.

Table 1. Characteristics of the Solid-State associations[a]

acceptor	anion	type	contacts	$d_{X\cdots C}$, Å[b]	R_{XC}[b]
DDQ	PF_6^-	1:1 chains	C···F	2.866	0.90
DDQ	BF_4^-	1:1 chains	C···F	2.849	0.90
DDQ	$CF_3SO_3^-$[c]	1:1 chains	C···O	2.766	0.86
DDQ	ClO_4^-[d]	1:1 chains	C···O	2.713	0.84
FA	PF_6^-	1:1 chains	C···F	2.919	0.92
FA	BF_4^-	2:1 complex	C···F	2.922	0.92
FA	ClO_4^-	2:1 complex	C···O	2.992	0.93
TCP	PF_6^-[e]	1:1 chains	C···F	2.958	0.93
TCP	BF_4^-[e]	1:1 chains[f]	[f]	[f]	[f]

[a] With Pr_4N^+, if not noted otherwise. [b] Shortest contact, $R_{XC} = d_{X\cdots C}/(r_X + r_C)$, where r_X and r_C are van der Waals radii.[56] [c] With Bu_4N^+. [d] With Bu_4N^+.[57] Note that co-crystals of DDQ with $(Pr_4N)ClO_4$, which were prepared in the current work showed disordered anions (see Figure S2 in the Supporting Information). [e] With $[K(cryptand)]^+$ counter-ions. [f] Disordered anions and TCP moieties.

Specifically, the $R_{XC} = d_{X\cdots C}/(r_X + r_C)$ values (which reflect, at least semi-quantitatively, the strength of the intermolecular interactions) for the associations with the fluoro- and oxoanions were in the 0.84–0.93 range. These values are similar to those in the previously reported associations of the same π-acceptors with the halide anions.[18,20] To compare thermodynamics and spectral properties of these complexes, we carried out UV–vis spectral measurements, as follows.

3.2. UV–vis Measurements of the Association of π-Acceptors with Fluoro- and Oxoanions. In agreement with the reported data,[18,20] addition of a salt of Cl^-, Br^- or I^- anions to the solution of any of the π-acceptors under study in dichloromethane resulted in the appearance of new intense absorption bands in the UV–vis spectrum (Figure 3A).

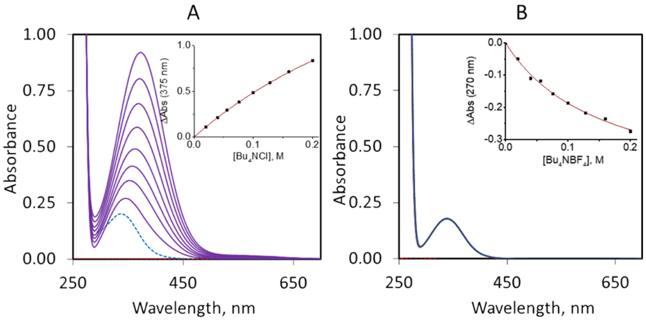

Figure 3. (A) UV–vis spectra (purple lines) of the solutions with constant concentration (10 mM) of FA and variable concentrations of Cl^- anions (from 20 to 200 mM). A spectrum of the individual FA is shown as a blue dashed line. (B) Overlapping UV–vis spectra of the solutions containing 10 mM of FA and various concentrations of BF_4^- (from 0 to 200 mM). Inserts: Fit of the differential absorptions at 380 (A) and 275 nm (B) to 1:1 binding isotherm.

The intensities of the new absorption bands were well fit by the 1:1 binding isotherm (insert in Figure 3A) corresponding to equilibrium in eq 1:

$$A + X^- \rightleftarrows A{\cdot}X^- \qquad (1)$$

where X^- is an anion and A is a π-acceptor. Such a fit produced *effective* formation constants of the complexes, K_{eff}, and extinction coefficients of the anion–π complexes (see Table S2 Supporting Information for details). In contrast to the halide anions, the UV–vis spectra of the solutions containing a π-acceptor and fluoro- or oxoanions seemed, at first glance, the same as that of the individual molecule (Figure 3B and Figures S6–S10 in the Supporting Information). Scrutiny of the spectra of the solutions containing oxo- or fluoroanions revealed, however, that the absorption bands of the π-acceptors were somewhat shifted or their shapes were slightly changed. For example, the intensity of the absorption in Figure 3B was decreasing in the 270–280 nm range with the increase of the concentration of BF_4^- anions in solution (Figure S6 in the Supporting Information). Analogous small increases or decreases of the absorption intensities in various spectral regions with the increase of concentration of oxo- or fluoroanions were observed for the solutions of TCP and DDQ (Figures S7–S10 in the Supporting Information). Similar to the solutions with halides, the differential absorptions, ΔAbs (obtained by the subtraction of the absorption of FA from the spectra of their mixtures) in the series of solutions with varied concentrations of anions were well fit by the 1:1 binding isotherms (insert in Figure 3B and Figures S7–S9 in the Supporting Information). Treatment of the data at different wavelengths produced consistent K_{eff} values for each anion/π-acceptor pair (Table S2 in the Supporting Information). It should be stressed, however, that these K_{eff} values were obtained using absorption data for the series of solutions with variable ionic strength (due to the variations in the concentration of anions). As such, the K_{eff} do not represent the true equilibrium constants (note that an addition of any other salts to maintain a constant ionic strength would introduce anions competing for the interaction with the π-acceptor, which would distort the resulting values of the formation constants). Still, the K_{eff} values obtained under analogous conditions can be used for the comparison of the tendency of the different anion/π-acceptor pairs to form anion–π complexes. Specifically, the K_{eff} values obtained for the complexes with oxo- and fluoroanions were in the same range (for the complexes with TCP or FA) as those obtained under the same conditions for the complexes with the halides. Thus, it indicated that the anion–π bonding between neutral π-acceptors and fluoro- and oxoanions is characterized by comparable strengths to that reported earlier for complexes with halides. Overall, the UV–vis measurements showed that thermodynamic characteristics of the complexes of the π-acceptors with fluoro-and oxoanions were, in general, comparable to those of the associations with halides. The spectral features of the complexes with these polyatomic and monoatomic anions were, however, quite different. To clarify the distinctions, if any, in the driving forces of the anion–π bonding with these two distinct types of anions, we turned to a computational analysis of these complexes.

3.3. Computational Analysis of the Anion–π Complexes: Spectra and Thermodynamics. Geometries of the complexes that resulted from the optimization of the anion–π complexes with halides, fluoro-, and oxoanions are illustrated in Figure 4 and Figure S11 in the Supporting Information.

In agreement with the reported X-ray structural data,[58] halides are located over the periphery of the π-acceptor rings in their optimized complexes. In particular, these monoatomic anions are positioned almost atop the carbonyl carbons of DDQ and FA or over the center of the C–C-carbon bonds of TCP (Figure 4 and Figure S10 in the Supporting Information). In comparison, the fluoro- and oxoanions are located closer to the center of the rings of the π-acceptors. In all these complexes, the distances between anions and one or several (in

https://doi.org/10.1021/acs.jpca.3c02704

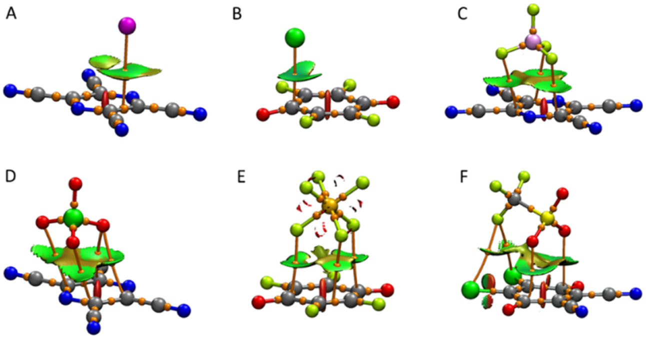

Figure 4. Superposition of the results of QTAIM and NCI analyses onto the optimized structures of TCP•I^- (A), FA•Cl^- (B), TCP•BF_4^- (C) TCP•ClO_4^- (D), FA•PF_6^- (E), and DDQ•$CF_3SO_3^-$ (F). The bond paths and critical (3, −1) points (from QTAIM) are shown as orange lines and spheres, and blue-green areas (from NCI) indicate bonding interactions; the atom color code is the same as in Figure 1.

the complexes with polyatomic anions) carbons of the rings are shorter than the sum of the corresponding van der Waals radii (Table S3 in the Supporting Information).

QTAIM analysis[48,49] of the complexes with halides confirmed the presence of one bond path and one (3,−1) critical bond point (BCP) between the anion and π-acceptor. In comparison, the complexes with the fluoro- and oxoanions showed multiple bond paths (and the corresponding BCPs) between counterparts. NCI analysis[50] confirmed the distinction between the single-point and multicenter interactions between π-acceptors and halide vs fluoro-/oxoanions, respectively (*vide infra*, also see previous work on the multicenter anion−π interaction[15]). As illustrated in Figure 4, NCI representations of the complexes show green areas (indicating attractive interaction between anions and π-acceptors) around each bond path and BCPs obtained from the QTAIM analysis.

The binding energies in the complexes with the oxo- and fluoroanions are comparable to that in the complexes with halides (Figure 5, see numerical values in Table S3 in the Supporting Information).

The interaction energies of each acceptor with all anions vary within the rather narrow range of about 4 kcal/mol, and the strength of the interaction with each anion increases from FA to TCP and DDQ. Following similar interaction energies, the R_{XC} values for the shortest interatomic contact in the complexes with the polyatomic anions are also close to those in complexes with halides (Figure 5). In complexes with each acceptor, R_{XC} values are decreasing in the order I > Br > Cl, and the values for the contacts of polyatomic anions are close to those with the intermediate complexes with bromide.

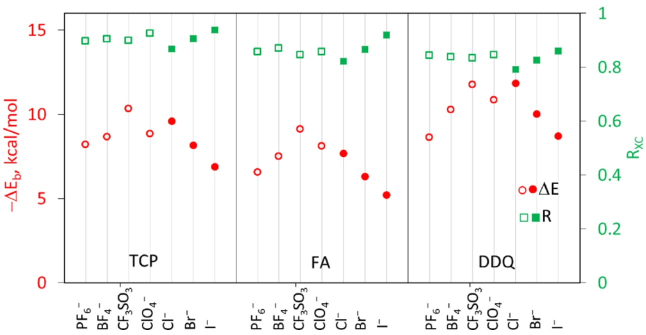

Figure 5. Variations of the ΔE_b (red circles) and R_{XC} values (green squares) in the anion−π complexes. Filled and open symbols represent pairs with halides and fluoro-/oxoanions, respectively.

While thermodynamic and structural characteristics in Figure 5 point to a similar strength of the anion−π bonding in the complexes with the polyatomic and monoatomic anions, the TD DFT calculations produced distinct UV−vis spectral features for these associations. Following the experimental data, the spectra of the complexes with the fluoro- and oxoanions were within 0.1−0.2 eV (Table 2) of those of the corresponding individual π-acceptor (the wavelength and extinction coefficients for all complexes and π-acceptors are listed in the Table S4 in the Supporting Information). In comparison, the calculated spectra of the complexes with halides comprise absorption bands with noticeably lower energies than the absorption bands of the corresponding π-acceptor, and the main component of the lowest-energy excited state involved a transition from the highest occupied molecular orbital (HOMO) of halide to the lowest unoccupied orbital (LUMO) of the acceptor. In agreement with the experimental data,[16,18] the energy of these bands in the complexes of the same π-acceptors decrease in the order Cl > Br > I. According to the Mulliken charge-transfer theory, it follows the increase of the energies of the HOMOs of the halides.[20,59] (Similar order of the absorption band energies was observed in halogen-bonded complexes of halide anions.[60])

Table 2. Energies of Absorption Bands Maxima ($h\nu$)[a] and Charge Transfer (Δq)[b] in the Anion−π Complexes

	TCP		FA		DDQ	
X^-	$h\nu$, eV	Δq, e	$h\nu$, eV	Δq, e	$h\nu$, eV	Δq, e
	4.96		5.11		3.28	
PF_6^-	4.92	0.01	5.08	0.01	3.41	0.01
BF_4^-	5.04	0.015	5.04	0.01	3.45	0.02
$CF_3SO_3^-$	5.04	0.02	5.02	0.01	3.48	0.02
ClO_4–	5.08	0.01	5.11	0.01	3.47	0.02
Cl^-	2.95	0.07	3.34	0.08	3.09	0.20
Br^-	2.71	0.06	2.93	0.10	2.71	0.20
I^-	2.35	0.05	2.44	0.06	2.28	0.22

[a] Lowest energy band (from TD DFT M062X/def2tzvpp calculations). [b] From NBO analysis.

Besides the appearance of the diagnostic absorption band, the formation of charge-transfer complexes is accompanied by the partial ground-state charge transfer from donor to acceptor related to their molecular−orbital interaction.[59] Indeed, the NBO analysis showed that complexes with halides are characterized by a value of charge-transfer, Δq, from anions to the π-acceptors in the range 0.05e−0.22e, and the values of Δq are highest in the complexes with DDQ, which is the strongest electron acceptor. The corresponding values calculated for the complexes with oxo- and fluoroanions are an order of magnitude lower (Table 2). These distinctions are apparently related to the differences in the energies and shapes of the molecular orbitals. In the framework of NBO, the stabilization (charge-transfer) energy, E_{CT}, is related to the interaction of the filled bonding orbital of the donor with the antibonding orbital of the acceptor. It can be approximated by second-order perturbative approach as $E_{CT} = 2F(i,j)^2/(\varepsilon_j - \varepsilon_i)$, where ε_i and ε_j are diagonal elements (energies of the interacting donor, i, and acceptor, j, orbitals), and $F(i,j)$ is the off-diagonal matrix element (which is a function of the orbital overlap).[47,61] Since the interaction of HOMO of anions with LUMO of the π-acceptors usually leads to the largest contribution to E_{CT}, an insight into the relative strength of charge-transfer bonding could be inferred from the consideration of the energies and shapes of these orbitals (Figure 6).

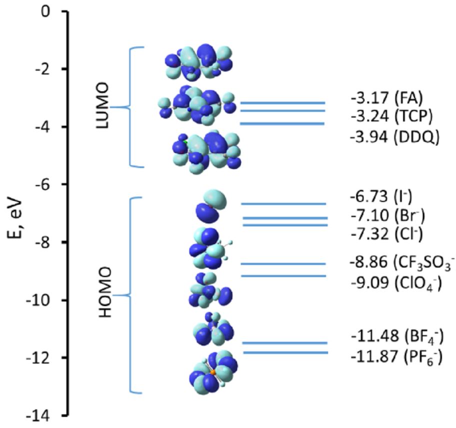

Figure 6. Frontier molecular orbital shapes and energies of the anions and π-acceptors.

It shows that the HOMO energies of halide anions are, on average, 3 eV higher than that of oxo- and fluoroanions. As a result, the energy gaps ($\varepsilon_j - \varepsilon_i$) for the complexes with oxo-and fluoroanions are about twice as large as those with halides. In addition, as was illustrated for complexes of halides with TCP,[58] shape of HOMOs and locations of the monoatomic halides over the π-acceptor are better suited for the efficient overlap with the LUMOs of acceptors than multi-fractional MOs of polyatomic oxo- and fluoroanions. The MO diagrams in Figure S11 in the Supporting Information confirm that molecular orbitals of the complex of FA with polyatomic perchlorate are largely localized either on the π-acceptor or on the anions (as such, the spectra of such complexes are close to the superposition of the spectra of components, *vide supra*). In comparison, some of the molecular orbitals of the FA·Br$^-$ complex are delocalized over both interaction species. As a result, the values of E_{CT} related to the interaction of the lone pair of the anion with the antibonding orbital of acceptor in the complexes with halides (e.g., 6.10 and 9.36 kcal/mol in FA·Br$^-$ and DDQ·Br$^-$, respectively) are much larger than in the complexes with oxo- and fluoroanions (e.g., 1.04 and 1.82 kcal/mol in FA·BF$_4^-$ and DDQ·BF$_4^-$, respectively). This leads to the substantial charge transfer and ground-state stabilization of the complexes with halides. It also indicates a partially covalent character of the anion−π interaction in complexes with halides (similar to the suggested earlier covalency in the anion−π complexes of Cl$^-$ with tetracyanobenzene[62] or flavine,[63] as well as in the halogen-bonded[64] and chalcogen-bonded[65] complexes.)

The energy decomposition analysis (EDA) clarified the distinctions between the nature of the complexes with oxo- and fluoroanions and those with the halides. Specifically, the EDA analysis using the AMS suite of programs decomposes the intermolecular interaction energy values into electrostatic, ΔE_{elstat}, Pauli repulsion, $\Delta E_{Pauli,}$ orbital (charge-transfer) interaction, ΔE_{oi} and dispersion, ΔE_{disp}, components:[53−55]

$$\Delta E_{int} = \Delta E_{elstat} + \Delta E_{Pauli} + \Delta E_{oi} + \Delta E_{disp} \qquad (2)$$

The values of ΔE_{int} and its components are listed in Table S5 in the Supporting Information. The variations in ΔE_{int} are following, in general, the binding energies, ΔE_b. For example, DDQ forms the strongest, on average, anion−π complexes among three π-acceptors, and the associations with chloride anions have the largest magnitudes of ΔE_{int} among the halide complexes with the same π-system. (Note that the absolute values of ΔE_b and ΔE_{int} for the same complex are different since the latter does not include reactants' deformation and solvation energies and they are calculated with the different functionals and basis sets). Most important for the current work, however, is the comparison of $\Delta E_{elstat,}$ ΔE_{oi}, and ΔE_{disp} in the associations with different anions and π-acceptors. Variations of the contributions (in %) of these components to the attractive interaction (e.g., % of $\Delta E_{elstat} = \Delta E_{elstat}/(\Delta E_{elstat} + \Delta E_{oi} + \Delta E_{disp}) \times 100\%$) and the comparable (relative) contributions of the repulsive Pauli energy, ΔP_{Pauli}, are illustrated in Figure 7.

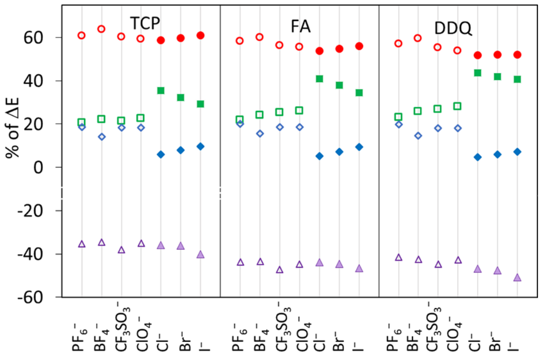

Figure 7. Contributions (in %) of ΔE_{elstat} (red circles), ΔE_{oi} (green squares), and ΔE_{disp} (blue rhombus) to the attractive interactions (the complexes with halides and fluoro-/oxoanions are shown with filled and open symbols, respectively). The corresponding contributions of the repulsive energy, ΔP_{Pauli}, are shown as purple triangles.

A glance at Figure 6 reveals that contributions of electrostatic attraction in the complexes of oxo- and fluoroanions with each π-acceptor are comparable to those in the associations with the halides. For complexes with oxo- and fluoroanions, contributions of ΔE_{oi} and ΔE_{disp} are also similar, and their magnitudes are about three times smaller than that of electrostatics. In the complexes with halides, however, the contributions of ΔE_{disp} are substantially lower than the contributions of ΔE_{oi}. The smaller contribution of ΔE_{disp} in complexes with monoatomic anions as compared to that in the associations with the polyatomic oxo- and fluoroanions anions is not surprising. It is noticeable, however, that the smaller contribution of ΔE_{disp} in the complexes with halides is compensated by the substantial increase of ΔE_{oi}. Moreover, the contributions of orbital interactions are increasing in the complexes with halides from TCP to FA and DDQ, while the contributions of electrostatics are decreasing slightly in the same order. As a result, the contribution of ΔE_{oi} in the complexes with the strongest electron acceptor, DDQ, is only about 20% lower than that of electrostatic interactions. The increase of orbital interaction is accompanied by some increase of the Pauli repulsion term (Figure 7 and Table S5 in the Supporting Information). Apparently, the closer arrangement of the anions to the carbon atoms of the ring led also to the more substantial repulsion of the filled orbitals of the interacting species.[66]

The substantial contribution of the molecular−orbital interaction explains the appearance of the intense charge-transfer absorption bands in the complexes with halide anions.[67] It also explains the structural features of the complexes with halides. Specifically, the most positive surface electrostatic potential (π-hole) is found over the center of the aromatic ring in tetracyanopyrazine.[59] However, instead of the arrangement over the π-hole, the halide anions are consistently located over the aromatic rings in a number of co-crystals of TCP (as well as tetracyanobenzene) with various stoichiometry and counter-ions.[17,18] Since the LUMOs of the π-acceptors are delocalized over the aromatic ring, it is thus the efficient mixing of the HOMOs of halides with the LUMOs of the π-acceptor, which governs the mutual arrangements of counterparts in these complexes.

4. CONCLUSIONS

The results of the experimental measurements in the solid state and solutions together with DFT calculations indicated that binding energies between the neutral π-acceptors and non-coordinating fluoro- and oxoanions are comparable to that with the halides. This similarity in binding energies resulted from the interplay of the contributions of the electrostatic, orbital, dispersion, and repulsive (Pauli) interactions. Yet, while the formation of the anion−π complexes with halides is accompanied by the appearance of the strong charge-transfer band (and substantial ground-state charge transfer), the complexes with the oxo- and fluoroanions are characterized by the negligible charge transfer and their UV−vis spectra are very similar to those of the individual π-acceptors. These distinctions in the spectral features are related to the differences in the energies and shapes of the HOMOs of the halides as compared to those of the oxo-and fluoroanions, as well as different arrangements of the anions in the respective complexes. Indeed, the classic works of Mulliken demonstrated that the energies and intensities of the in the absorption bands of the molecular complexes are determined primarily by the energies and efficient interaction between the frontier molecular orbital of the reactants.[59,67] The shapes and lower energy of HOMOs and over-the-rim arrangements of the monoatomic halides (over carbonyl carbons in the complexes with FA or DDQ or close to the middle of C-C bond in associations with TCP) allow the efficient overlap with the LUMO of the π-acceptors (and delocalization of the MO of the complexes over both counter-parts). In comparison, due to the arrangement of the polyatomic fluoro- and oxoanions closer to the center of the π-acceptors and the lower energies and multi-segment shapes of their HOMOs, the orbital interactions in these complexes are less efficient (so their MOs remain mostly localized on either anion or π-acceptor). In accordance with these results, EDA pointed out that complexes of neutral π-acceptors with the polyatomic fluoro- and oxoanions are formed predominantly via electrostatic attractions. Interaction energies in similar associations with the halide anions comprise significant contributions of orbital interactions. The higher contributions of the orbital interactions is counterbalanced by the decrease of the contributions of dispersion interactions in the complexes with halides as compared to the associations with the polyatomic anions (while the contributions of electrostatic attraction and Pauli repulsion did not change significantly with the change of the anions). In the complexes with the strongest π-acceptors, the covalent (charge-transfer) interactions are comparable in strength to those of electrostatics. The significant orbital interactions lead to the appearance of strong charge-transfer bands in the spectra of the complexes with halides. They also explain the consistent arrangements of the halides over the periphery of the TCP aromatic ring (which facilitates HOMO/LUMO interactions), instead of over the center of the aromatic ring, which is characterized by the highest surface electrostatic potentials. This finding further underlines that besides structural distinctions, variations of the anions and π-acceptors leads to substantial differences in the nature of the interaction in the anion−π complexes.

■ ASSOCIATED CONTENT

Supporting Information

The Supporting Information is available free of charge at https://pubs.acs.org/doi/10.1021/acs.jpca.3c02704.

> Experimental (crystallographic and UV−vis spectral) data, as well as details of calculations of formation constants and computations of interaction energies, and results of EDA analyses of the anion−π complexes (PDF)

■ AUTHOR INFORMATION

Corresponding Author

Sergiy V. Rosokha − *Department of Chemistry, Ball State University, Muncie, Indiana 47306, United States;* orcid.org/0000-0003-3172-8523; Email: svrosokha@bsu.edu

Authors

Favour E. Odubo − *Department of Chemistry, Ball State University, Muncie, Indiana 47306, United States*
Matthias Zeller − *Department of Chemistry, Purdue University, West Lafayette, Indiana 47907, United States;* orcid.org/0000-0002-3305-852X

Complete contact information is available at:
https://pubs.acs.org/10.1021/acs.jpca.3c02704

Notes

The authors declare no competing financial interest.

■ ACKNOWLEDGMENTS

We thank the National Science Foundation (grant CHE-2003603) for the financial support of this work. Calculations were done on Ball State University's beowulf cluster, which is supported by the National Science Foundation (MRI-1726017), and Ball State University. X-ray measurements were supported by the National Science Foundation through the Major Research Instrumentation Program under grant no. CHE 1625543 (funding for the single crystal X-ray diffractometer).

■ REFERENCES

(1) Quinonero, D.; Garau, C.; Rotger, C.; Frontera, A.; Ballester, P.; Costa, A.; Deya, P. M. Anion-π interactions: Do they exist? *Angew. Chem., Int. Ed.* **2002**, *41*, 3389−3392.

(2) Mascal, M.; Armstrong, A.; Bartberger, M. D. Anion-aromatic bonding: a case for anion recognition by π-acidic rings. *J. Am. Chem. Soc.* **2002**, *124*, 6274−6276.

(3) Alkorta, I.; Rozas, I.; Elguero, J. Interaction of anions with perfluoro aromatic compounds. *J. Am. Chem. Soc.* **2002**, *124*, 8593−8598.

(4) Schottel, B. L.; Chifotides, H. T.; Dunbar, K. R. Anion-π interactions. *Chem. Soc. Rev.* **2008**, *37*, 68−83.

(5) Ballester, P. Experimental Quantification of anion−π interactions in solution using neutral host−guest model systems. *Acc. Chem. Res.* **2013**, *46*, 874−884.

(6) Quinonero, D.; Frontera, A.; Deya, P. M. Anion-π interactions in molecular recognition. In *Anion Coordination Chemistry*, Bowman-James, K.; Bianchi, A.; Garcia-Espana, E. Eds. 2011, 321−361.

(7) Mareda, J.; Matile, S. Anion−π slides for transmembrane transport. *Chem. − Eur. J.* **2009**, *15*, 28−37.

(8) Wang, D.-X.; Wang, M.-X. Exploring anion−π interactions and their applications in supramolecular chemistry. *Acc. Chem Res.* **2020**, *53*, 1364−1380.

(9) Giese, M.; Albrecht, M.; Rissanen, K. Experimental investigation of anion-π interactions - applications and biochemical relevance. *Chem. Commun.* **2016**, *52*, 1778−1795.

(10) Zhao, Y.; Cotelle, Y.; Liu, L.; López-Andarias, J.; Bornhof, A.-B.; Akamatsu, M.; Sakai, N.; Matile, S. The emergence of anion−π catalysis. *Acc. Chem. Res.* **2018**, *51*, 2255−2263.

(11) Bauzá, A.; Mooibroek, T. J.; Frontera, A. The bright future of unconventional σ/π-hole interactions. *ChemPhysChem* **2015**, *16*, 2496−2517.

(12) Wheeler, S. E.; Houk, K. N. Are anion/π interactions actually a case of simple charge-dipole interactions? *J. Phys. Chem. A* **2010**, *114*, 8658−8664.

(13) Thirman, J.; Head-Gordon, M. Efficient Implementation of energy decomposition analysis for second-order Møller−Plesset perturbation theory and application to anion−π interactions. *J. Phys. Chem. A* **2017**, *121*, 717−728.

(14) Kozuch, S. Should "Anion−π interactions" be called "anion−σ interactions"? A revision of the origin of some hole-bonds and their nomenclature. *Phys. Chem. Chem. Phys.* **2016**, *18*, 30366−30369.

(15) Foroutan-Nejad, C.; Badri, Z.; Marek, R. Multi-center covalency: revisiting the nature of anion−π interactions. *Phys. Chem. Chem. Phys.* **2015**, *17*, 30670−30679.

(16) Wilson, J.; Maxson, T.; Wright, I.; Zeller, M.; Rosokha, S. V. Diversity and uniformity in anion-π complexes of thiocyanate with aromatic, olefinic and quinoidal π-acceptors. *Dalton Trans.* **2020**, *49*, 8734−8743.

(17) Berryman, O. B.; Bryantsev, V. S.; Stay, D. P.; Johnson, D. W.; Hay, B. P. Structural criteria for the design of anion receptors: the interaction of halides with electron-deficient arenes. *J. Am. Chem. Soc.* **2007**, *129*, 48−58.

(18) Rosokha, Y. S.; Lindeman, S. V.; Rosokha, S. V.; Kochi, J. K. Halide recognition through diagnostic "anion-π " interactions: molecular complexes of Cl-, Br-, and I- with olefinic and aromatic π-receptors. *Angew. Chem., Int. Ed.* **2004**, *43*, 4650−4652.

(19) Chifotides, H. T.; Schottel, B. L.; Dunbar, K. R. The π-accepting arene HAT(CN)6 as a halide receptor through charge transfer: multisite anion interactions and self-assembly in solution and the solid state. *Angew. Chem., Int. Ed.* **2010**, *49*, 7202−7207.

(20) Kepler, S.; Zeller, M.; Rosokha, S. V. Anion−π complexes of halides with p-benzoquinones: structures, thermodynamics, and criteria of charge transfer to electron transfer transition. *J. Am. Chem. Soc.* **2019**, *141*, 9338−9348.

(21) Milasinovic, V.; Vukovic, V.; Krawczuk, A.; Molcanov, K.; Hennig, C.; Bodensteiner, M. The nature of π-hole interactions between iodide anions and quinoid rings in the crystalline state. *IUCrJ* **2023**, *10*, 156−163.

(22) Han, B.; Lu, J.; Kochi, J. K. anion recognitions via cocrystallizations with organic π-acids in the efficient self-assembly of nanoscopic one-dimensional molecular chains (wires). *Cryst. Growth Des.* **2008**, *8*, 1327−1334.

(23) Rosokha, S. V.; Kumar, A. Anion-π interaction in metal-organic networks formed by metal halides and tetracyanopyrazine. *J. Mol. Struct.* **2017**, *1138*, 129−135.

(24) Kuzniak-Glanowska, E.; Kobylarczyk, J.; Jedrzejowska, K.; Glosz, D.; Podgajny, R. Exploring the structure-property schemes in anion-π systems of d-block metalates. *Dalton Trans.* **2021**, *50*, 10999−11015.

(25) Wang, D.-X.; Wang, M.-X. Anion−π interactions: generality, binding strength, and structure. *J. Am. Chem. Soc.* **2013**, *135*, 892−897.

(26) Kim, D.; Tarakeshwar, P.; Kim, K. S. Theoretical investigations of anion-π interactions: the role of anions and the nature of pi systems. *J. Phys. Chem. A* **2004**, *108*, 1250−1258.

(27) Bagwill, C.; Anderson, C.; Sullivan, E.; Manohara, V.; Murthy, P.; Kirkpatrick, C. C.; Stalcup, A.; Lewis, M. Predicting the strength of anion-pi interactions of substituted benzenes: the development of anion-π binding substituent constants. *J. Phys. Chem. A* **2016**, *120*, 9235−9243.

(28) Bauza, A.; Quinonero, D.; Deya, P. M.; Frontera, A. Theoretical ab initio study of anion-π interactions in inorganic rings. *Chem. Phys. Lett.* **2012**, *530*, 145−150.

(29) Luo, J.; Zhu, J.; Tuo, D.-H.; Yuan, Q.; Wang, L.; Wang, X.-B.; Ao, Y.-F.; Wang, Q.-Q.; Wanea, D.-X. Macrocycle-directed construction of tetrahedral anion-π receptors for nesting anions with complementary geometry. *Chem.- Eur. J.* **2019**, *25*, 13275−13279.

(30) Caramori, G. F.; Ostrom, I.; Ortolan, A. O.; Nagurniak, G. R.; Besen, V. M.; Munoz-Castro, A.; Orenha, R. P.; Parreira, R. L. T.; Galembeck, S. E. The usefulness of energy decomposition schemes to rationalize host-guest interactions. *Dalton Trans.* **2020**, *49*, 17457−17471.

(31) Savastano, M.; Bazzicalupi, C.; Giorgi, C.; García-Gallarín, C.; López de la Torre, M. D.; Pichierri, F.; Bianchi, A.; Melguizo, M. Anion complexes with tetrazine-based ligands: formation of strong anion−π interactions in solution and in the solid State. *Inorg. Chem.* **2016**, *55*, 8013−8024.

(32) Rosokha, S. V.; Lu, J.; Han, B.; Kochi, J. K. Unusual structural effects of intermolecular π-bonding in the tetracyanopyrazine (ion-radical) dimer. *New J. Chem.* **2009**, *33*, 545−553.

(33) Kuzniak, E.; Hooper, J.; Srebro-Hooper, M.; Kobytarczyk, J.; Dziurka, M.; Musielak, B.; Pinkowicz, D.; Raya, J.; Fertay, S.; Podgajny, R. A Concerted evolution of supramolecular interactions in a {cation; metal complex; π-acid; solvent} anion-π system. *Inorg. Chem. Front.* **2020**, *7*, 1851−1863.

(34) Molčanov, K.; Mali, G.; Grdadolnik, J.; Stare, J.; Stilinović, V.; Kojić-Prodić, B. iodide···π interactions of perhalogenated quinoid rings in co-crystals with organic bases. *Cryst. Growth Des.* **2018**, *18*, 5182−5193.

(35) Howe, D.; Wilson, J.; Rosokha, S. V. Solvent and ionic atmosphere effects in anion-π interactions: complexes of halide anions with p-benzoquinones. *J. Phys. Chem. A.* **2022**, *126*, 4255−4263.

(36) *Bruker Apex3 v2016.9−0, SAINT V8.37A*; Bruker AXS Inc.: Madison, WI, 2016.

(37) Sheldrick, G. *SHELXTL suite of programs,* Version 6.14, 2000-2003, Bruker AXS Inc.: Madison, WI, 2003.

(38) Sheldrick, G. Crystal Structure Refinement with SHELXL. *Acta Cryst. C* **2015**, *71*, 3−8.

(39) Hübschle, C. B.; Sheldrick, G. M.; Dittrich, B. ShelXle: a Qt Graphical User Interface for SHELXL. *J. Appl. Crystallogr.* **2011**, *44*, 1281−1284.

(40) *Gaussian 09*, Revision C.01, M. J., Frisch; G. W., Trucks; H. B., Schlegel; G. E., Scuseria; M. A., Robb; J. R., Cheeseman; G., Scalmani; V., Barone; B., Mennucci; Petersson, H. G. A. et al., Gaussian, Inc.: Wallingford CT, 2009.

(41) Zhao, Y.; Truhlar, D. G. The M06 suite of density functionals for main group thermochemistry, thermochemical kinetics, noncovalent interactions, excited states, and transition elements: two new functionals and systematic testing of four M06-class functionals and 12 other functionals. *Theor. Chem. Acc.* **2008**, *120*, 215−241.

(42) Weigend, F.; Ahlrichs, R. Balanced basis sets of split valence, triple zeta valence and quadruple zeta valence quality for H to Rn: Design an assessment of accuracy. *Phys. Chem. Chem. Phys.* **2005**, *7*, 3297−3305.

(43) Tomasi, J.; Mennucci, B.; Cammi, R. Quantum mechanical continuum solvation models. *Chem. Rev.* **2005**, *105*, 2999.

(44) Zhu, Z.; Xu, Z.; Zhu, W. Interaction nature and computational methods for halogen bonding: a perspective. *J. Chem. Inf. Model.* **2020**, *60*, 2683.

(45) Wang, K.; Lv, J.; Miao, J. Assessment of density functionals and force field methods on anion−π interaction in heterocyclic calix complexes. *Theor. Chem. Acc.* **2015**, *134*, 5.

(46) Bauzá, A.; Quiñonero, D.; Deyà, P. M.; Frontera, A. Is the use of diffuse functions essential for the properly description of noncovalent interactions involving anions? *J. Phys. Chem. A* **2013**, *117*, 2651−2655.

(47) Weinhold, F.; Landis, C. R. *Discovering Chemistry with Natural Bond Orbitals,* Wiley, Hoboken, New Jersey, 2012, DOI: 10.1002/9781118229101.

(48) Bader, R. F. W. A quantum theory of molecular structure and its applications. *Chem. Rev.* **1991**, *91*, 893−928.

(49) Popelier, P. L. A. *The QTAIM perspective of chemical bonding in The Chemical Bond*, John Wiley & Sons, Ltd, 2014, p. 271.

(50) Johnson, E. R.; Keinan, S.; Mori-Sánchez, P.; Contreras-García, J.; Cohen, A. J.; Yang, W. Revealing noncovalent interactions. *J. Am. Chem. Soc.* **2010**, *132*, 6498−6506.

(51) Lu, T.; Chen, F. Multiwfn: A Multifunctional Wavefunction Analyzer. *J. Comput. Chem.* **2012**, *33*, 580−592.

(52) Humphrey, W.; Dalke, A.; Schulten, K. VMD − Visual Molecular Dynamics. *J. Mol. Graphics* **1996**, *14*, 33−38.

(53) Bickelhaupt, F. M.; Baerends, E. J. Kohn-Sham density functional theory: predicting and understandding chemistry. In *Reviews in Computational Chemistry*; John Wiley & Sons, Ltd, 2007; pp. 1−86.

(54) Baerends, E. J.; Ziegler, T.; Autschbach, J.; Bashford, D.; Berger, A.; Bérces, A.; Bickelhaupt, F. M.; Bo, C.; de Boeij, P. L.; Boerrigter, P. M.; Borini, S. et al. *ADF2012.01*; SCM: Amsterdam, 2012.

(55) te Velde, G.; Bickelhaupt, F. M.; Baerends, E. J.; Fonseca Guerra, C.; van Gisbergen, S. J. A.; Snijders, J. G.; Ziegler, T. Chemistry with ADF. *J. Comput. Chem.* **2001**, *22*, 931−967.

(56) Bondi, A. van der Waals Volumes and Radii. *J. Phys. Chem.* **1964**, *68*, 441−451.

(57) de Boer, J. A. A.; Reinhoudt, D. N.; Uiterwijk, J. W. H. M.; Harkema, S. Synthesis, X-Ray crystal structure, and reactivity of ternary complexes of crown ethers, organic π-acceptors, and salts. *J. Chem. Soc., Perkin Trans. 2* **1986**, *3*, 377−381.

(58) Grounds, O.; Zeller, M.; Rosokha, S. V. Structural preferences in strong anion-π and halogen-bonded complexes: π- and σ-holes vs frontier orbitals interaction. *New J. Chem.* **2018**, *42*, 10572−10583.

(59) Mulliken, R.S.; Person, W. B. Molecular Complexes. *A Lecture and Reprint Volume* Wiley: New York, 1969.

(60) Rosokha, S. V.; Traversa, A. From charge transfer to electron transfer in halogen-bonded complexes of electrophilic bromocarbons with halide anions. *Phys. Chem. Chem. Phys.* **2015**, *17*, 4989−4999.

(61) Reed, A. E.; Curtiss, L. A.; Weinhold, F. Intermolecular interactions from a natural bond orbital, donor-acceptor viewpoint. *Chem. Rev.* **1988**, *88*, 899−926.

(62) Novotný, J.; Bazzi, S.; Marek, R.; Kozelka, J. Lone-Pair−π Interactions: Analysis of the Physical Origin and Biological Implications. *Phys. Chem. Chem. Phys.* **2016**, *18*, 19472−19481.

(63) Yurenko, Y. P.; Bazzi, S.; Marek, R.; Kozelka, J. Anion-Pi Interactions in Flavoproteins Involve a Substantial Charge-Transfer Component. *Chem.-Eur. J.* **2017**, *23*, 3246−3250.

(64) Torubaev, Y. V.; Howe, D.; Leitus, G.; Rosokha, S. V. The relationship between the crystal habit and the energy framework pattern: a case study involving halogen bonding on the edge of a covalent bond. *CrystEngComm* **2023**, *25*, 3380−3390.

(65) Bora, P. L.; Novák, M.; Novotný, J.; Foroutan-Nejad, C.; Marek, R. Supramolecular Covalence in Bifurcated Chalcogen Bonding. *Chem. − Eur. J.* **2017**, *23*, 7315−7323.

(66) Jakobsche, C. E.; Choudhary, A.; Miller, S. J.; Raines, R. T. (N → Π* Interaction and n)(π Pauli Repulsion Are Antagonistic for Protein Stability). *J. Am. Chem. Soc.* **2010**, *132*, 6651−6653.

(67) Anslyn, E. V.; Dougherty, D. A. *Modern Physical Organic Chemistry*; University Science Books: Sausalito, California, 2006, p. 186.